MNRAS **434,** 1469–1475 (2013)
Advance Access publication 2013 July 16
doi:10.1093/mnras/stt1105

ExoMol line lists – II. The ro-vibrational spectrum of SiO

Emma J. Barton,* Sergei N. Yurchenko and Jonathan Tennyson
Department of Physics and Astronomy, University College London, London WC1E 6BT, UK

Accepted 2013 June 17. Received 2013 June 15; in original form 2013 May 26

ABSTRACT

Accurate rotational–vibrational line lists are calculated for silicon monoxide. Line lists are presented for the main isotopologue, $^{28}Si^{16}O$, and for four monosubstituted isotopologues ($^{29}Si^{16}O$, $^{30}Si^{16}O$, $^{28}Si^{18}O$ and $^{28}Si^{17}O$), in their ground electronic states. These line lists are suitable for high temperatures (up to 9000 K), including those relevant to exoplanetary atmospheres and cool stars. A combination of empirical and *ab initio* methods is used: the potential energy curves are determined to high accuracy by fitting to extensive data from the analysis of both laboratory and sunspot spectra; a high-quality *ab initio* dipole moment curve is calculated at the large basis set, multireference configuration interaction level. A partition function plus full line lists of rotational–vibrational transitions are made available in an electronic form as Supplementary Information to this article and at www.exomol.com.

Key words: molecular data – opacity – astronomical data bases: miscellaneous – planets and satellites: atmospheres – stars: low-mass.

1 INTRODUCTION

Silicon monoxide (SiO) is a widely observed astronomical species and appears to be ubiquitous in our Galaxy. Since its initial detection by Snyder & Buhl (1974), SiO has proved to be a key astrophysical maser and its very bright maser emissions are the subject of continued study (Assaf et al. 2011; Cotton, Ragland & Danchi 2011; Deguchi et al. 2011; Nakashima et al. 2011; Vlemmings, Humphreys & Franco-Hernandez 2011).

SiO was originally detected in the interstellar medium by Wilson et al. (1971). Its emissions were subsequently observed in the envelopes of oxygen-rich giant and supergiant stars (Kaifu, Buhl & Snyder 1975) and the remnants of Supernova 1987A (Aitken et al. 1988). SiO was detected in absorption in cool giant stars (Rinsland & Wing 1982), including α Tau (Cohen et al. 1992). SiO absorptions are prominent in sunspots which have proved to be a fruitful source of spectroscopic data on highly excited states (Glenar et al. 1985; Campbell et al. 1995) which we exploit below. Furthermore, recent detections of hot, dense exoplanets have led to the speculation that their atmospheres might contain significant quantities of SiO from vapourized silicates (Schaefer, Lodders & Fegley 2012).

These astronomical applications, combined with technological uses of SiO spectra (Wooldridge, Danczyk & Wu 2000; Motret et al. 2002), have motivated a number of laboratory studies. Tipping & Chackerian (1981, hereafter TC), Mollaaghababa et al. (1991), Campbell et al. (1995), Cho & Saito (1998) and Sanz, McCarthy & Thaddeus (2003) have all produced molecular constants characterizing SiO rotational–vibrational (ro-vibrational) states. Transition probabilities or Einstein A coefficients have also been provided by TC, Langhoff & Bauschlicher (1993) and Drira et al. (1998). Transition line lists have been constructed using these data (Lovas, Maki & Olson 1981; Glenar et al. 1985; Langhoff & Bauschlicher 1993; Drira et al. 1998), but none of them appears to be particularly complete. For example, no single line list combines a comprehensive set of transition frequencies with an accurate model for the transition intensities. It is this that we aim to do here.

TC reported transition probabilities for a large number of transitions based on a semi-empirical dipole moment which they claim should give results accurate to about 10 per cent. Langhoff & Bauschlicher (1993) computed an accurate electric dipole moment function for the SiO molecule which not only reproduces accurate dipole moments, but also reproduces line strengths for ro-vibrational transitions within the ground state manifold. The resulting line lists are for $^{28}Si^{16}O$, $^{29}Si^{16}O$ and $^{30}Si^{16}O$ for $J \leq 250$, but v is limited to 15. Intensities were calculated using band intensities and Hönl–London factors. Drira et al. (1998) calculated an *ab initio* $^{28}Si^{16}O$ line list for $J \leq 100$ and $v \leq 40$, although the publicly available line list from the Strasbourg Data Centre contains only 503 transitions. Drira et al.'s (1998) intensities are significantly larger than those of TC and they estimate their intensities are only accurate to about 20 per cent.

The ExoMol project (Tennyson & Yurchenko 2012) aims to provide line lists of spectroscopic transitions for key molecular species which are likely to be important in the atmospheres of extrasolar planets and cool stars; its aims, scope and methodology have been summarized by Tennyson & Yurchenko (2012). Line lists for $^2\Sigma^+$ XH molecules, $X =$ Be, Mg, Ca, have already been published (Yadin et al. 2012). In this paper, we present ro-vibrational transition lists and associated spectra for the five major isotopologues of SiO.

* E-mail: emma.barton.09@ucl.ac.uk

These line lists are particulary comprehensive and should be valid for temperatures up to 9000 K.

2 METHOD

Ro-vibrational line lists for the ground electronic state of SiO were obtained by direct solution of the nuclear motion Schrödinger equation using the program LEVEL 8.0 (Le Roy 2007). In principle, the calculations were initiated using a potential energy curve (PEC) calculated *ab initio*. In practice, as detailed below, there are sufficient experimental data available for SiO that the PEC was actually characterized by fitting to these data using the program DPOTFIT 1.1 (Le Roy 2006).

2.1 Dipole moments

There appears to be no experimental measurement of any SiO transition dipoles and a single measurement of its permanent dipole moment as a function of the vibrational state by Raymonda, Muenter & Klemperer (1970). We determined a new dipole moment curve (DMC) using high-level *ab initio* calculations. These are compared to previous high-level *ab initio* determinations (Langhoff & Bauschlicher 1993; Drira et al. 1998; Chattopadhyaya, Chattopadhyay & Das 2003) given below.

The *ab initio* calculations were performed using MOLPRO (Werner et al. 2010); we tested both the coupled cluster (CCSD(T)) and multireference configuration interaction (MRCI) methods with large basis sets. Our largest, and best, calculations used an aug-cc-pCV5Z basis set for the CCSD(T) study and aug-cc-pwCV5Z for MRCI; in both cases, a correction due to the correlation of the core electrons was included, but the corresponding correction due to relativistic effects was found to be very small and was neglected. These calculations give a value for the dipole at equilibrium of 3.10 D and 3.07 D, respectively, which bracket the experimentally determined value of 3.088 D (Raymonda et al. 1970). The *ab initio* DMC grid points were used directly in LEVEL.

Fig. 1 compares the DMCs arising from our calculations with those obtained by Chattopadhyaya et al. (2003, hereafter CCK) using an MRCI method. Other previous studies based on the use of a similar CCSD(T) method gave curves similar to our CCSD(T) calculation. The CCSD(T) dipoles appear correct at short bond lengths but behave in an unphysical fashion for $R > 2$ Å. CCSD(T) is known to have problems as molecules are dissociated and so this model was not pursued. Again at short R our MRCI dipoles are similar to those of CCK. It is unclear why CCK's dipoles do not vary smoothly as R is increased, but such behaviour is not consistent with obtaining reliable transition intensities. All calculations presented below therefore use our MRCI dipole moments.

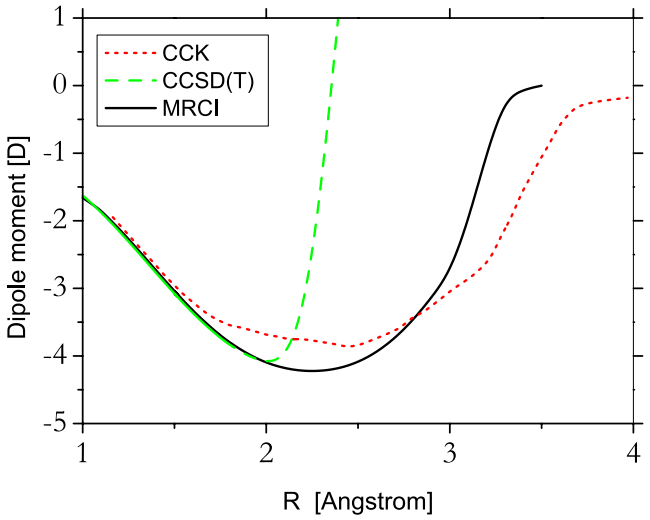

Figure 1. *Ab initio* DMCs for SiO in its ground electronic state. MRCI and CCSD(T) are *ab initio* calculations performed as part of this work; CCK is the MRCI dipole of CCK.

2.2 Fitting the potential

The PEC is essentially characterized by fitting to spectroscopic data. Measurements with very small estimated uncertainties were chosen for the fit such that any uncertainty in the fitted surface depends only on the accuracy of the fit and, for higher energies, the extrapolation beyond the experimental input values. Measurements for multiple isotopologues were used both to maximize the input data and to ensure that the resulting curve is applicable to all isotopologues, including the yet-to-be-observed spectrum of $^{28}Si^{17}O$. The most comprehensive and accurate sets of available measurements are the infrared ro-vibrational sunspot lines detected by Campbell et al. (1995) and the microwave rotational laboratory lines recorded by Sanz et al. (2003) (see Table 1).

The potential was expressed as an extended Morse oscillator potential function:

$$V(r) = D_e \left[1 - e^{-\phi(r)(r-r_e)}\right]^2, \quad (1)$$

where

$$\phi(r) = \sum_{i=0}^{N} \phi_i y_p(r, r_e)^i, \quad (2)$$

$$y_p(r, r_e) = \frac{r^p - r_e^p}{r^p + r_e^p}, \quad (3)$$

and p was set to 2 and N to 6. Spectroscopically derived values for the dissociation energy, $D_e = 66\,620.0$ cm^{-1} (Campbell et al. 1995) and $r_e = 1.509\,7377$ Å (Sanz et al. 2003), were used.

Data for isotopologues were fitted simultaneously; attempts to include Born–Oppenheimer Breakdown terms in the fit did not result in an improvement and were not pursued. Of the 1816 lines used in the fit, 1294 were $^{28}Si^{16}O$, 301 were $^{29}Si^{16}O$, 178 were $^{30}Si^{16}O$ and 43 were $^{28}Si^{18}O$. These data were used to determine seven constants with values for r_e and D_e held fixed. Fits were started from an *ab initio* PEC but were not sensitive to this starting point. The resulting fits reproduced the input experimental data within 0.01 cm^{-1} and often, particularly for the pure rotational data, much better than this. Parameters resulting from the fit are given in Table 2.

2.3 Partition function

A partition function for $^{28}Si^{16}O$ was calculated by summing all the calculated energy levels (see Section 3) using Excel. As we use all ro-vibrational energy levels, there are no issues with the convergence of this sum. Given the high accuracy of our energy levels, this determination should be more accurate than the previous determinations given by Irwin (1981) and Sauval & Tatum (1984). Table 3 compares with these previous studies and finds generally good agreement, except the values of Sauval & Tatum (1984) become too large at higher temperatures.

Table 1. Summary of observation data used to determine the SiO PEC. Temperatures are only approximate and the uncertainties are the estimates given in the cited papers.

Reference	Method	Transition	Temperature (K)	Frequency range (cm^{-1})	Uncertainty (cm^{-1})
Sanz et al. (2003)	Laboratory	$\Delta v = 0, J' \rightarrow J'' = 1 \rightarrow 0$ $^{28}Si^{16}O$ $v = 0$–45 $^{29}Si^{16}O$ $v = 0$–26 $^{28}Si^{18}O$ $v = 0$–44	1000–9000	0.13–1.67	6.7×10^{-8}
Campbell et al. (1995)	Sunspots	$\Delta v = 1, \Delta J = \pm 1$ $^{28}Si^{16}O$ $v = 0$–13, $J \leq 141$ $^{29}Si^{16}O$ $v = 0$–6, $J \leq 107$ $^{30}Si^{16}O$ $v = 0$–6, $J \leq 92$	3200	900–1300	0.006

Table 2. Fitting parameters used in the extended Morse oscillator potential (see equation 1). (Uncertainties are given in parentheses in units of the last digit.)

N	ϕ_i
0	1.868 690 70(93)
1	− 0.142 883(30)
2	0.188 883(98)
3	0.2255(14)
4	0.1959(37)
5	− 0.471(16)
6	2.714(29)

Table 3. Comparison of $^{28}Si^{16}O$ partition functions.

T (K)	This work	Sauval & Tatum (1984)	Irwin (1981)
1000	1163.1	1169.2	1164.2
2000	3319.0	3316.1	3322.0
3000	6638.3	6618.3	6639.8
4000	11 172.6	11 000.2	11 164.1
5000	16 976.3	16 629.7	16 937.5
6000	24 109.4	23 833.9	24 002.6
7000	32 640.8	33 080.1	32 403.5
8000	42 648.8	44 989.4	42 186.6
9000	54 221.8	60 371.5	53 401.1

For ease of use, we fitted our partition function, Q, to a series expansion of the form used by Vidler & Tennyson (2000):

$$\log_{10} Q(T) = \sum_{n=0}^{6} a_n \left[\log T\right]^n \quad (4)$$

with the values given in Table 4.

2.4 Line-list calculations

Line lists were calculated for the five isotopologues $^{28}Si^{16}O$, $^{29}Si^{16}O$, $^{30}Si^{16}O$, $^{28}Si^{18}O$ and $^{28}Si^{17}O$. All ro-vibrational states were considered and transitions satisfying the dipole selection rule $\Delta J = \pm 1$. A summary of each line list is given in Table 7. These line lists in principle span frequencies up to 65 000 cm^{-1}; in practice, transitions above 10 000 cm^{-1} are very weak.

The procedure described above was used to produce line lists, i.e. catalogues of transition frequencies $\tilde{\nu}_{ij}$ and Einstein coefficients A_{ij}, for five SiO isotopologues: $^{28}Si^{16}O$, $^{29}Si^{16}O$, $^{30}Si^{16}O$, $^{28}Si^{18}O$ and $^{28}Si^{17}O$. The computed line lists for the five isotopologues are available in an electronic form as Supplementary Information to this article.

3 RESULTS

The line lists contain almost two million transitions each and are therefore, for compactness and ease of use, divided into separate energy levels and transition files. This is done using the standard ExoMol format (Tennyson, Hill & Yurchenko 2013) which is based on a method originally developed for the BT2 line list (Barber et al. 2006). Extracts for the start of the $^{28}Si^{16}O$ files are given in Tables 5 and 6. The full line list for each of these isotopologues are summarised in Table 7. They can be downloaded from the CDS via http://cdsarc.u-strasbg.fr/pub/cats/J.MNRAS.htx. The line lists and partition function together with auxiliary data, including the potential parameters and dipole moment functions, as well as the absorption spectrum given in cross-section format (Hill, Yurchenko & Tennyson 2013), can all be obtained from there as well as from www.exomol.com.

Table 8 compares our SiO line lists with previous attempts to study this system: it only provides an assessment of the quantity of data provided, not its quality. However, it is clear that our new line lists provide a much more comprehensive coverage of the problem.

Table 4. Fitting parameters used to fit the partition functions (see equation 4). Fits are valid for temperatures between 900 and 9000 K.

	$^{28}Si^{16}O$	$^{29}Si^{16}O$	$^{30}Si^{16}O$	$^{28}Si^{18}O$	$^{28}Si^{17}O$ [a]	
a_0	−4.289 479 066	−2.645 361 792	−4.290 451 186	−4.296 319 774	9.147 577 169	−3.273 169 177
a_1	7.197 126 92	4.920 534 06	7.196 400 21	7.191 459 85	2.344 430 76	12.276 769 29
a_2	−1.356 461 55	0.251 599 71	−1.356 028 88	−1.355 139 10	−12.161 294 65	3.084 956 99
a_3	−1.506 716 29	−2.112 020 57	−1.504 903 51	−1.496 841 90	9.009 934 87	−9.935 504 66
a_4	0.909 814 866	1.038 226 161	0.909 249 889	0.905 530 086	−2.947 037 343	4.767 331 120
a_5	−0.182 925 0025	−0.197 500 4943	−0.182 902 8096	−0.182 305 6408	0.470 855 3438	−0.908 900 4600
a_6	0.012 906 6948	0.013 598 5360	0.012 911 1795	0.012 878 7601	−0.029 961 4057	0.062 633 7008

[a]Left-hand column: $T \leq 4700$ K; right-hand column: $T > 4700$ K.

Table 5. Extract from the state files for $^{28}Si^{16}O$. Full tables are available at http://cdsarc.u-strasbg.fr/cgi-bin/VizieR?-source=J/MNRAS/. The files contain 24 306 entries for $^{28}Si^{16}O$, 25 254 for $^{28}Si^{17}O$, 26 162 for $^{28}Si^{18}O$, 24 617 for $^{29}Si^{16}O$ and 24 915 for $^{30}Si^{16}O$.

I	$\tilde{E}$	g	J	v
1	0.000 000	1	0	0
2	1.448 467	3	1	0
3	4.345 384	5	2	0
4	8.690 712	7	3	0
5	14.484 267	9	4	0
6	21.726 203	11	5	0
...	...	...	...	...

I: state counting number; $\tilde{E}$: state energy in cm^{-1}; g: state degeneracy; J: state rotational quantum number; v: state vibrational quantum number.

Table 6. Extracts from the transition files for $^{28}Si^{16}O$. Full tables are available at http://cdsarc.u-strasbg.fr/cgi-bin/VizieR?-source=J/MNRAS/. The files contain 178 4964 entries for $^{28}Si^{16}O$, 189 0039 for $^{28}Si^{17}O$, 199 3 414 for $^{28}Si^{18}O$, 181 8923 for $^{29}Si^{16}O$ and 185 2656 for $^{30}Si^{16}O$.

I	F	A_{IF}
2	1	2.8438E−06
3	2	2.7301E−05
4	3	9.8720E−05
5	4	2.4265E−04
6	5	4.8470E−04
7	6	8.5037E−04
...	...	...

I: upper state counting number; F: lower state counting number; A_{IF}: Einstein A coefficient in s^{-1}.

Table 7. Summary of our SiO line lists.

	$^{28}Si^{16}O$	$^{29}Si^{16}O$	$^{30}Si^{16}O$	$^{28}Si^{18}O$	$^{28}Si^{17}O$
Maximum v	95	95	96	98	97
Maximum J	408	410	413	423	416
Number of lines	1784 964	1818 923	1852 656	1993 414	1890 039

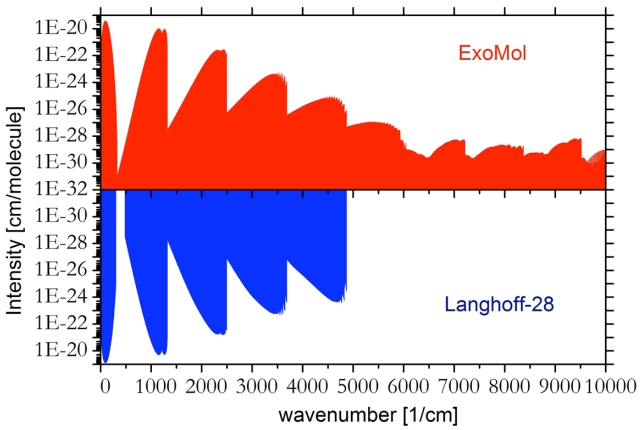

Figure 2. Absorption spectra of $^{28}Si^{16}O$ at $T = 296$ K: ExoMol versus Langhoff & Bauschlicher (1993).

We believe they also represent a substantial improvement in accuracy. Fig. 2 gives a room temperature comparison of our $^{28}Si^{16}O$ line list with the most complete previous one due to Langhoff & Bauschlicher (1993). It is clear our line list is more complete.

Illustrative high-resolution comparisons with $^{28}Si^{16}O$-observed sunspot transition frequencies are given in Table 9; as can be seen, the comparison is excellent. Also given are the frequencies due to Langhoff & Bauschlicher (1993), who generated a PEC from the empirical parameters of Glenar et al. (1985); again, the comparison is very good. Overall the error in Langhoff & Bauschlicher's frequencies, where available, is only about twice ours.

An important aim in fitting the PEC is to also predict spectroscopic data for higher vibrational states than used in the fit. To test this, comparisons are made with the experimentally derived vibrational frequencies of Shanker, Linton & Verma (1976), which have an estimated uncertainty of 1.0 cm^{-1}, and of Bredohl et al. (1973), as re-assigned by Barrow & Stone (1975) (see Table 10). Our predictions agree well with the experimentally derived values; however, those of TC disagree significantly for the higher vibrational states. Indeed by $v = 35$ our vibrational term value is 3.3 cm^{-1} lower than TC's. TC were limited in the vibrational states they could use in their fit, extending only to $v = 5$ from the spectra of Lovas et al. (1981), compared to the line frequencies for vibrational transitions used which extend to $v = 13$.

Since there are no measured intensities to compare with, we compare the results of our calculations with astronomical spectra. Sunspots display many SiO features over a wide range of wavelengths. High-resolution sunspot spectra have been compiled by Wallace et al. (1996). Fig. 3 compares small regions of these spectra with our line lists. Note that only the theoretical spectra, generated at $T = 3200$ K, are given in the absolute units of cm molecule^{-1}.

Table 8. Summary comparison of SiO ro-vibrational line lists. Given are the isotopologues considered, the maximum values for vibrational (v) and rotational (J) states considered, the maximum change in vibrational state (Δv), whether intensity information and a partition function are provided.

Reference	Lovas et al. (1981)	Glenar et al. (1985)	Langhoff & Bauschlicher (1993)	Drira et al. (1997)	This work
Isotopes	1	3	3	1	5
maximum v	6	10	15	40	98
maximum J	98	86	250	1	423
maximum Δv	2	1	4	3	98
Intensities?	No	No	Yes	Yes	Yes
Partition function?	No	No	No	No	Yes

Table 9. Comparison of theoretically predicted ro-vibrational wavenumbers, in cm^{-1}, with the high-resolution sunspot observed of Campbell et al. (1995).

J'	J''	v'	v''	Observation	This work		Langhoff & Bauschlicher (1993)	
					Calculated	Observed−Calculated	Calculated	Observed−Calculated
9	10	1	0	1214.6810	1214.6829	−0.0019	1214.68	0.00
9	10	2	1	1202.8878	1202.8876	0.0002	1202.89	−0.00
9	10	3	2	1191.1305	1191.1291	0.0014	1191.13	0.00
9	10	4	3	1179.4093	1179.4070	0.0023	1179.41	−0.00
9	10	8	7	1132.8751	1132.8725	0.0026	1132.87	0.01
9	10	10	9	1109.8133	1109.8123	0.0010	1109.81	0.00
9	10	11	10	1098.3324	1098.3329	−0.0005	1098.33	0.00
9	10	13	12	1075.4744	1075.4740	0.0004	1075.48	−0.01
11	10	2	1	1232.8767	1232.8735	0.0032	1232.87	0.01
11	10	3	2	1220.9058	1220.9040	0.0018	1220.91	−0.00
11	10	4	3	1208.9734	1208.9711	0.0023	1208.97	0.00
11	10	5	4	1197.0759	1197.0742	0.0017	1197.08	−0.00
11	10	6	5	1185.2130	1185.2129	0.0001	1185.21	0.00
11	10	7	6	1173.3880	1173.3867	0.0013	1173.39	−0.00
11	10	8	7	1161.5964	1161.5954	0.0010	1161.60	−0.00
11	10	10	9	1138.1158	1138.1155	0.0003	1138.12	−0.00
10	11	1	0	1213.1327	1213.1350	−0.0023	1213.13	0.00
10	11	2	1	1201.3510	1201.3499	0.0011	1201.35	0.00
10	11	3	2	1189.6031	1189.6015	0.0016	1189.60	0.00
10	11	5	4	1166.2155	1166.2135	0.0020	1166.21	0.01
10	11	6	5	1154.5742	1154.5727	0.0015	1154.57	0.00
10	11	7	6	1142.9704	1142.9668	0.0036	1142.97	0.00
10	11	9	8	1119.8600	1119.8586	0.0014	1119.86	0.00
10	11	12	11	1085.4509	1085.4502	0.0007	1085.45	0.00
10	11	13	12	1074.0547	1074.0474	0.0073	1074.05	0.00
125	126	2	1	965.1065	965.1051	0.0014	965.09	0.02
125	126	3	2	954.5828	954.5856	−0.0028	954.57	0.01
125	126	4	3	944.0942	944.0980	−0.0038	944.09	0.00
126	127	1	0	973.1300	973.1257	0.0043	973.11	0.02
126	127	2	1	962.5855	962.5854	0.0001	962.57	0.02
126	127	4	3	941.5952	941.6004	−0.0052	941.59	0.01
127	128	1	0	970.5914	970.5876	0.0038	970.57	0.02
127	128	2	1	960.0589	960.0585	0.0004	960.04	0.02
127	128	3	2	949.5598	949.5612	−0.0014	949.55	0.01
127	128	4	3	939.0904	939.0956	−0.0052	939.08	0.01
128	129	1	0	968.0462	968.0425	0.0037	968.03	0.02
128	129	2	1	957.5253	957.5244	0.0009	957.51	0.02
128	129	3	2	947.0347	947.0382	−0.0035	947.02	0.01
129	130	2	1	954.9832	954.9833	−0.0001	954.97	0.01
130	131	1	0	962.9348	962.9306	0.0042	962.91	0.02
130	131	2	1	952.4351	952.4349	0.0002	952.42	0.02
130	131	3	2	941.9681	941.9710	−0.0029	941.95	0.02
131	132	1	0	960.3668	960.3641	0.0027	960.35	0.02
131	132	2	1	949.8787	949.8795	−0.0008	949.86	0.02
131	132	3	2	939.4210	939.4266	−0.0056	939.41	0.01
132	133	1	0	957.7940	957.7905	0.0035	957.77	0.02
132	133	2	1	947.3225	947.3171	0.0054	947.30	0.02
132	133	3	2	936.8721	936.8753	−0.0032	936.85	0.02
134	135	2	1	942.1713	942.1709	0.0004	942.15	0.02
135	136	2	1	939.5876	939.5874	0.0002	939.56	0.03
136	137	1	0	947.4301	947.4255	0.0046	947.40	0.03
137	138	1	0	944.8216	944.8167	0.0049	944.79	0.03
137	138	2	1	934.3987	934.3992	−0.0005	934.37	0.03
139	140	2	1	929.1778	929.1832	−0.0054	929.15	0.03
140	141	1	0	936.9546	936.9489	0.0057	936.92	0.03
140	141	2	1	926.5650	926.5649	0.0001	926.53	0.04

Table 10. Comparison of theoretically predicted vibrational spacings, in cm^{-1}, with the low-resolution experiments of Bredohl et al. (1973) for $13 \leq v \leq 17$, and Bredohl et al. (1973), as re-assigned by Barrow & Stone (1975), for $23 \leq v \leq 28$.

$v' - v''$	Observed	Calculated This work	Observed−Calculated This work	TC
14 − 13	1078.5	1077.72	0.8	0.8
15 − 14	1067.0	1066.27	0.7	0.7
16 − 15	1055.0	1054.86	0.1	0.1
17 − 16	1044.0	1043.48	0.5	0.4
18 − 17	1033.0	1032.13	0.9	0.8
24 − 23	964.69	964.70	−0.01	−0.36
25 − 24	953.55	953.58	−0.03	−0.04
26 − 25	942.28	942.48	−0.20	−0.03
27 − 26	931.37	931.41	−0.04	−0.52
28 − 27	920.22	920.38	−0.16	−0.74

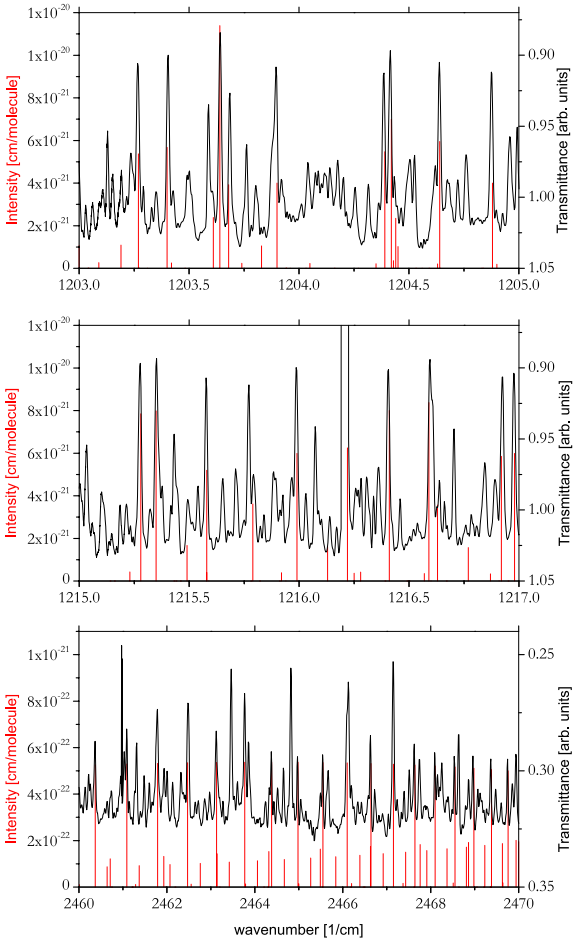

Figure 3. Sunspot absorption spectra (Wallace et al. 1996) (continuous line) and our predicted $^{28}Si^{16}O$ absorptions at 3200 K (vertical lines). The absolute intensity scale refers to the calculated spectra.

These spectra, chosen to cover regions where Δv is both 1 and 2, illustrate the excellent agreement between our line positions and the observed features. Our intensities are also well correlated with the observed ones. We note that the sunspot spectra show many other features in this figure. These features are either due to water (Polyansky et al. 1997) or due to some so-far-unidentified species.

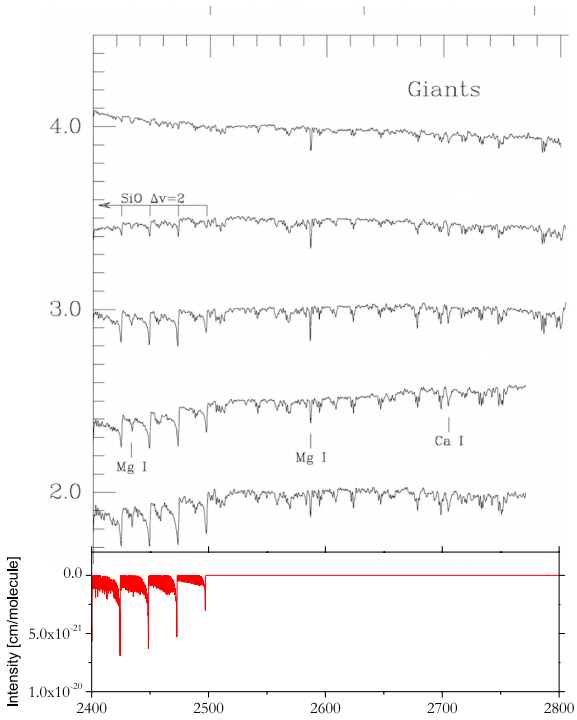

Figure 4. Red giant spectra due to Wallace & Hinkle (2002) compared to a synthesized $^{28}Si^{16}O$ absorption spectrum using $T = 3200$ K (bottom panel).

Fig. 4 compares the spectra of four red giants (Wallace & Hinkle 2002) with our simulated spectrum of $^{28}Si^{16}O$ at a temperature of 3200 K. These spectra are for the $\Delta v = 2$ overtone spectrum. To fully reproduce the observed stellar spectrum would require running a stellar model which is beyond the scope of this paper. However, it is clear that both the line positions and general band structure predicted by our calculations are in very good agreement with the observations.

4 CONCLUSIONS

We present comprehensive line lists for the five most important isotopologues of SiO. These are based on the direct solution of the nuclear motion Schrödinger equation using a PEC obtained by fitting to an extensive data set of measured transitions. These data are reproduced to near-experimental accuracy, resulting in high-accuracy line positions. A new *ab initio* dipole moment is computed, which appears to behave more physically at large internuclear separations. This dipole is used to compute Einstein *A* coefficients for all possible dipole-allowed transitions within each SiO isotopologue. The result is a comprehensive line list for each species, including the first data for $^{28}Si^{17}O$. The line lists can be downloaded from the CDS via ftp://cdsarc.u-strasbg.fr/pub/cats/J/MNRAS/, or from http://cdsarc.u-strasbg.fr/viz-bin/qcat?J/MNRAS/, or from www.exomol.com.

ACKNOWLEDGEMENTS

This work is supported by ERC Advanced Investigator Project 267219.

REFERENCES

Aitken D. K., Smith C. H., James S. D., Roche P. F., Hyland A. R., McGregor P. J., 1988, MNRAS, 231, 7

Assaf K. A., Diamond P. J., Richards A. M. S., Gray M. D., 2011, MNRAS, 415, 1083
Barber R. J., Tennyson J., Harris G. J., Tolchenov R. N., 2006, MNRAS, 368, 1087
Barrow R. F., Stone T. J., 1975, J. Phys.B: At. Mol. Opt. Phys., 8, L13
Bredohl H., Cornet R., Dubois I., Remy F., 1973, Can. J. Phys., 51, 2332
Campbell J. M., Klapstein D., Dulick M., Bernath P. F., 1995, ApJS, 101, 237
Chattopadhyaya S., Chattopadhyay A., Das K. K., 2003, J. Mol. Struct.: THEOCHEM, 639, 177 (CCK)
Cho S. H., Saito S., 1998, ApJ, 496, L51
Cohen M., Witteborn F. C., Carbon D. F., Augason G., Wooden D., Bregman J., Goorvitch D., 1992, AJ., 104, 2045
Cotton W. D., Ragland S., Danchi W. C., 2011, ApJ, 736, 96
Deguchi S., Koike K., Kuno N., Matsunaga N., Nakashima J.-i., Takahashi S., 2011, PASJ, 63, 309
Drira I., Hure J. M., Spielfiedel A., Feautrier N., Roueff E., 1997, A&A, 319, 720
Drira I., Spielfiedel A., Edwards S., Feautrier N., 1998, J. Quant. Spectrosc. Radiat. Transfer, 60, 1
Glenar D. A., Hill A. R., Jennings D. E., Brault J. W., 1985, J. Mol. Spectrosc., 111, 403
Hill C., Yurchenko S. N., Tennyson J., 2013, Icarus, preprint (arXiv:1205.6514)
Irwin A. W., 1981, ApJS, 45, 621
Kaifu N., Buhl D., Snyder L., 1975, ApJ, 195, 359
Langhoff S. R., Bauschlicher C. W., 1993, Chem. Phys. Lett., 211, 305
Le Roy R. J., 2006, DPotFit 1.1. A Computer Program for Fitting Diatomic Molecule Spectral Data to Potential Energy Functions. University of Waterloo Chemical Physics Research Report CP-662R (http://leroy.uwaterloo.ca/programs/)
Le Roy R. J., 2007, LEVEL 8.0. A Computer Program for Solving the Radial Schrödinger Equation for Bound and Quasibound Levels. University of Waterloo Chemical Physics Research Report CP-663 (http://leroy.uwaterloo.ca/programs/)
Lovas F. J., Maki A. G., Olson W. B., 1981, J. Mol. Spectrosc., 87, 449
Mollaaghababa R., Gottlieb C. A., Vrtilek J. M., Thaddeus P., 1991, ApJ, 368, L19
Motret O., Coursimault F., Viladrosa R., Pouvesle J. M., 2002, High Temp. Mater. Process., 6, 305
Nakashima J.-I., Deguchi S., Imai H., Kemball A., Lewis B. M., 2011, ApJ, 728, 76
Polyansky O. L., Zobov N. F., Viti S., Tennyson J., Bernath P. F., Wallace L., 1997, Sci, 277, 346
Raymonda J. W., Muenter J. S., Klemperer W. A., 1970, J. Chem. Phys., 52, 3458
Rinsland C. P., Wing R. F., 1982, ApJ, 262, 201
Sanz M. E., McCarthy M. C., Thaddeus P., 2003, J. Chem. Phys., 119, 11715
Sauval A. J., Tatum J. B., 1984, ApJS, 56, 193
Schaefer L., Lodders K., Fegley B., Jr, 2012, ApJ, 755, 41
Shanker R., Linton C., Verma R. D., 1976, J. Mol. Spectrosc., 60, 197
Snyder L. E., Buhl D., 1974, ApJ, 189, L31
Tennyson J., Yurchenko S. N., 2012, MNRAS, 425, 21
Tennyson J., Hill C., Yurchenko S. N., 2013, AIP Conf. Proc., Eighth International Conference on Atomic and Molecular Data and Their Applications. Am. Inst. Phys., New York
Tipping R. H., Chackerian C., 1981, J. Mol. Spectrosc., 88, 352 (TC)
Vidler M., Tennyson J., 2000, J. Chem. Phys., 113, 9766
Vlemmings W. H. T., Humphreys E. M. L., Franco-Hernandez R., 2011, ApJ, 728, 149
Wallace L., Hinkle K., 2002, AJ., 124, 3393
Wallace L., Livingston W., Hinkle K., Bernath P., 1996, ApJS, 106, 165
Werner H. J., Knowles P. J., Lindh R., Manby F. R., Schütz M., 2010, MOLPRO, A Package of Ab Initio Programs (http://www.molpro.net/)
Wilson R. W., Penzias A. A., Jefferts K. B., Kutner M., Thaddeus P., 1971, ApJ, 167, L97
Wooldridge M. S., Danczyk S. A., Wu J. F., 2000, J. Quant. Spectrosc. Radiat. Transfer, 64, 573
Yadin B., Vaness T., Conti P., Hill C., Yurchenko S. N., Tennyson J., 2012, MNRAS, 425, 34

This paper has been typeset from a TEX/LATEX file prepared by the author.